

Enantioselective Catalytic Dearomative Addition of Grignard Reagents to 4-Methoxypyridinium Ions

Yafei Guo, Marta Castiñeira Reis, Johanan Kootstra, and Syuzanna R. Harutyunyan*



Cite This: *ACS Catal.* 2021, 11, 8476–8483



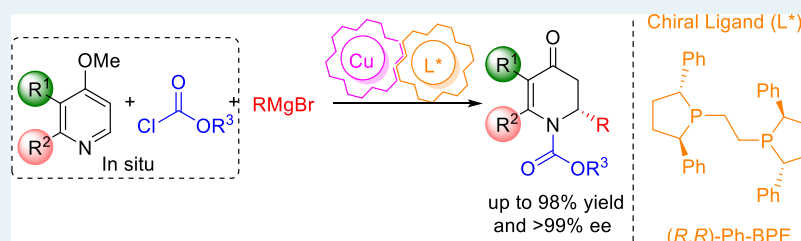
Read Online

ACCESS |

Metrics & More

Article Recommendations

Supporting Information



ABSTRACT: We describe a general catalytic methodology for the enantioselective dearomative alkylation of pyridine derivatives with Grignard reagents, allowing direct access to nearly enantiopure chiral dihydro-4-pyridones with yields up to 98%. The methodology involves dearomatization of in situ-formed *N*-acylpyridinium salts, employing alkyl organomagnesium reagents as nucleophiles and a chiral copper (I) complex as the catalyst. Computational and mechanistic studies provide insights into the origin of the reactivity and enantioselectivity of the catalytic process.

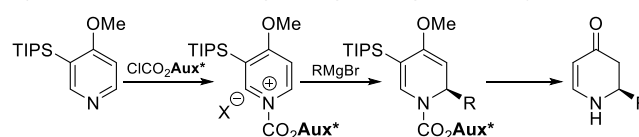
KEYWORDS: dihydro-4-pyridones, dearomatization, organomagnesium reagents, acylpyridiniums, copper catalysis

Pyridine and its derivatives are among the most significant heterocyclic units. Not only are they found in the structures of many natural products and pharmaceuticals but they also serve as building blocks for constructing other common scaffolds such as six-membered aza-heterocycles.¹ Prime examples are dihydropyridine and piperidine motives, which are ubiquitous in numerous alkaloids and bioactive molecules. As a result, extensive work has been directed toward the synthesis of chiral dihydropyridine and piperidine derivatives.^{2,3}

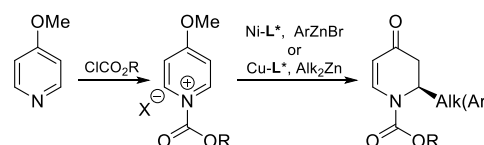
Several methodologies relying on the conjugate addition of organometallics to pyridine and dihydropyridones (commonly synthesized from the corresponding pyridine-based precursors) have been reported to date.⁴ At the same time, elegant strategies that depend on the direct use of pyridinium salts as substrates in addition reactions have been reported as well.^{5,6} Among literature precedence, the strategy that makes use of Grignard reagents and relies on chiral pyridinium salts to control the stereochemistry of the addition step has found the broadest application and still remains the preferred option (Scheme 1A).⁵ On the other hand, catalytic examples that make use of prochiral acylpyridinium ions are especially attractive in terms of atom economy and cost-efficiency. As a result, several catalytic methods that utilize prochiral acylpyridinium ions have also been reported,⁶ including nickel-catalyzed arylations^{6h,i} and copper-catalyzed alkylations,^{6j} both using organozinc reagents (Scheme 1B). While highly enantiopure products can be obtained using these strategies, both reports are restricted to unsubstituted pyridine

Scheme 1. State of the Art in Asymmetric Dearomatization of Acylpyridinium Ions with Organometallics

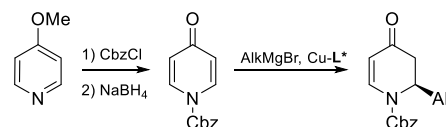
A) Stereoselective addition of Grignard reagents using chiral auxiliary



B) Catalytic enantioselective alkylation and arylation using organozinc reagents



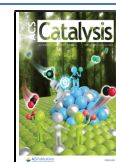
C) Catalytic enantioselective additions to pyridones prepared from 4-Methoxypyridine



Received: April 4, 2021

Revised: June 16, 2021

Published: June 28, 2021



or 4-methoxypyridine and make use of expensive zinc reagents. Furthermore, the alkylation protocol suffers from a limited scope of nucleophiles and low yields.^{6j}

Grignard reagents are one of the most attractive organometallics in terms of their availability, cost-efficiency, and reactivity. However, the high reactivity of both acylpyridinium ions and Grignard reagents leads to fast non-catalyzed background reactions, which results in racemic products and is difficult to outcompete for a chiral catalyst. As a result, the only known example that makes use of Grignard reagents relies on stereoselective synthesis using acylpyridinium ions and a chiral auxiliary. Recently, we reported the enantioselective catalytic synthesis of chiral dihydro-4-pyridones via asymmetric addition of Grignards to pyridones, the low reactivity of which is beneficial to achieve asymmetric induction in catalytic conditions (Scheme 1C).⁴ⁱ Despite good yields and excellent enantioselectivities, this procedure has its own drawbacks: the substrate must be prepared from 4-MeO-pyridines in two low yielding additional steps and, as in the case of the abovementioned catalytic additions of organozinc reagents, this methodology is limited to a single pyridone substrate.

Herein, we disclose a highly enantioselective catalytic dearomatization of in situ-generated *N*-acylpyridinium salts using highly reactive Grignard reagents and a chiral copper catalyst. What sets this method apart is the use of readily available Grignard reagents, a broader scope that includes substituted pyridines, and operational simplicity. This allows straightforward access to enantioenriched derivatives of dihydropyridone, enabling the further generation of multiple stereocenters.

We started off our investigations using 4-methoxypyridine **1a** as the starting material, phenyl chloroformate as the acylating agent, and EtMgBr as the Grignard reagent (Table 1). Anticipating a background reaction between the highly reactive acylpyridinium ion and the Grignard reagent, we chose $-78\text{ }^{\circ}\text{C}$ as the reaction temperature for the optimization studies. First, we investigated the rate of the uncatalyzed reaction in different solvents, namely, THF, Et₂O, and toluene. In all cases, full conversion of **1a** to the addition product **2a** was observed (entry 1), indicating that a catalyst with very high turnover frequency is needed to outcompete the uncatalyzed addition reaction. Based on our recent experience in combining copper catalysis with Grignard reagents,^{4i,7} we employed a Cu (I) salt as a potential catalyst for this reaction. In the presence of CuBr·SMe₂ (5 mol %), full conversion to the product was obtained in THF, but to our surprise, no product was formed when performing the reaction in toluene or Et₂O (entries 3–4). A subsequent ligand screening in combination with CuBr·SMe₂ involved a variety of commercially available chiral ligands **L1**–**L7**, including bidentate ferrocenyl- and biaryl-based diphosphines and monodentate phosphoramidite. The only chiral ligand that showed promising results in combination with the Cu (I) salt was diphosphine ligand **L1**. While using **L1** in combination with a copper salt in THF still results in racemic **2a**, some enantioenrichment (37% ee) was observed when the reaction was carried out in 2-Me-THF (entries 5 and 6). Moreover, when the reaction was performed in other solvents (Et₂O, CH₂Cl₂, and toluene, entries 7–9), the **L1**-Cu (I) catalyst system provided good results with full conversion to product **2a** and enantiomeric excess (ee) values between 88 and 94%. In contrast, the catalytic system with bidentate ligands **L2**–**L6** provided racemic products, whereas monodentate **L7** gave no

Table 1. Optimization of Reaction Conditions for the Addition of EtMgBr to 4-Methoxypyridine **1a**^a

entry	L-Cu (I) ^b	solvent	Conv. (%) ^c	ee (%) ^d
1		THF, Et ₂ O, toluene	full	
2	Cu (I)	THF	full	0
3	Cu (I)	toluene	0	
4	Cu (I)	Et ₂ O	0	
5	L1 -Cu (I)	THF	full	0
6	L1 -Cu (I)	2-Me-THF	full	37
7	L1 -Cu (I)	Et ₂ O	full	88
8	L1 -Cu (I)	toluene	full	94
9	L1 -Cu (I)	CH ₂ Cl ₂	full	93

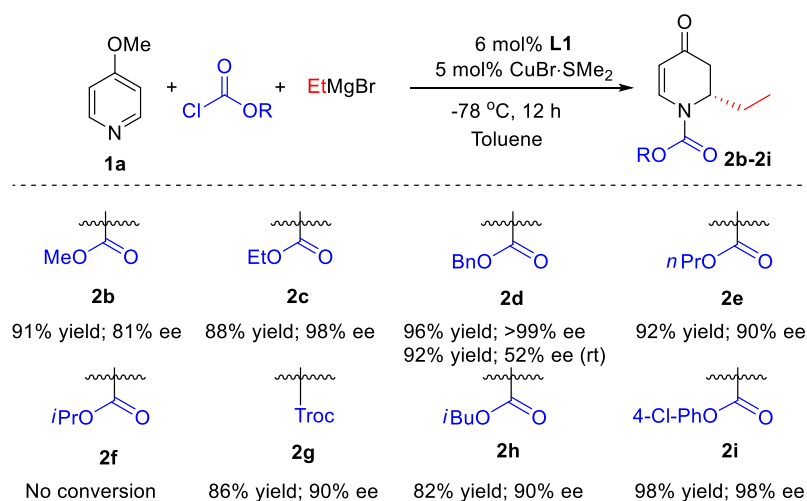
^aReaction conditions: 4-methoxypyridine **1a** (0.2 mmol), phenylchloroformate (2.0 equiv), and EtMgBr (2.0 equiv), in solvent (2 mL) at $-78\text{ }^{\circ}\text{C}$, for 12 h. ^bLigand **L** (6 mol %), CuBr·SMe₂ (5 mol %). ^cConversions were determined by ¹H NMR. ^dThe ee was determined by HPLC on a chiral stationary phase.

conversion. Consequently, we adopted the following reaction conditions as the optimal ones for further studies: **L1** (6 mol %), CuBr·SMe₂ (5 mol %), and Grignard reagent (2.0 equiv) in toluene at $-78\text{ }^{\circ}\text{C}$ for 12 h (entry 8).

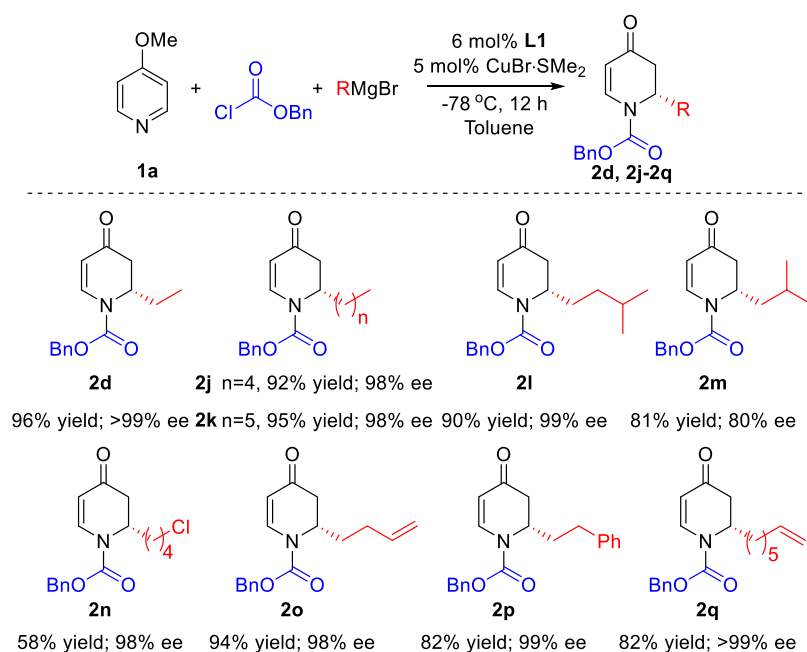
With the optimized conditions in hand, we investigated the scope of the reaction with respect to the acylating reagents (Scheme 2). With the exception of isopropyl chloroformate, for which the corresponding product **2f** was not formed, all tested acylating reagents, including aliphatic and aromatic chloroformates, provided high isolated yields (82 to 98%) and enantioselectivities (81 to >99% ee).

The reaction using benzyl chloroformate, for which product (**2d**) was obtained with the highest ee at $-78\text{ }^{\circ}\text{C}$ (>99%), was also attempted at room temperature. The increase in the reaction temperature was detrimental for the stereoselectivity, with the enantiomeric purity decreasing from >99% to 52%.

Based on the described results, benzyl chloroformate was selected as the acylating reagent for the investigation of the scope of Grignard reagents. We were pleased to find that a wide variety of alkyl Grignards, including β - and γ -branched reagents, were tolerated and gave the corresponding products (**2d**, **2j**–**m**) with good yields and high ees (Scheme 3). The addition of secondary Grignard reagents (cyclopentyl and isopropyl magnesium bromide), however, led to the racemic products. Various functionalized Grignard reagents were also evaluated which delivered their corresponding products (**2n**–

Scheme 2. Scope of Acylating Reagents^a

^aReaction conditions are the same as in Table 1 using different acylating agents. The reported yields correspond to isolated yields.

Scheme 3. Scope of Grignard Reagents^a

^aReaction conditions are the same as in Table 1 using different Grignard reagents. The reported yields correspond to isolated yields.

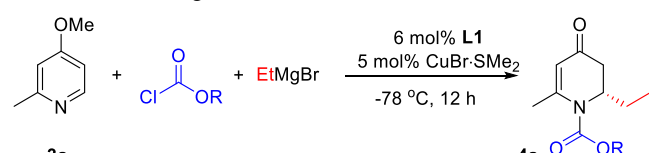
2q) with moderate to high yields (58–94%) and ees exceeding 98%.

The next important question to assess was whether derivatives of 4-methoxypyridine are amenable to our catalytic system because if successful, this would represent a straightforward route to chiral precursors that are highly valuable for generating molecules with multiple stereocenters. Literature precedence reveals that the substituted derivatives of 4-methoxypyridine are often not successful candidates for nucleophilic additions due to a diminished tendency to form pyridinium ions, which is crucial for the reactivity toward nucleophiles. We opted for the addition of EtMgBr to 4-methoxy-2-methylpyridine 3a as a model reaction under the optimal reaction conditions found for substrate 1a (Table 1, entry 8). However, under these conditions, no conversion was observed. Suspecting that the steric hindrance introduced by

the additional substituent might impede the pyridinium salt formation, we decided to exchange benzyl chloroformate for methyl chloroformate to stimulate the formation of pyridinium ions.

Optimization of the reaction conditions with this substrate revealed that a synthetically useful yield (66%) of the desired addition product with 97% ee can be obtained with CH₂Cl₂ as the solvent (Table 2, compare entry 3 with entries 2 and 4–7).

On the other hand, in the same solvent, no substrate conversion was observed for benzyl and phenyl acylpyridinium salts (entries 8–9). Encouraged by these results, we synthesized several 2-substituted 4-methoxypyridine substrates and evaluated them in the reaction with EtMgBr (Scheme 4), obtaining addition products with various alkyl substituents (4a–d) with decent yields (51–66%) and good to high enantioselectivities (80–97%).

Table 2. Optimization of Reaction Conditions for the Addition of EtMgBr to 3a^a


entry	R	solvent	yield (%) ^b	ee (%) ^c
1	Bn	toluene	0	Nd
2	Me	THF	<10	13
3	Me	CH ₂ Cl ₂	66	97
4	Me	Et ₂ O	15	82
5	Me	2-Me-THF	15	31
6	Me	toluene	<5	Nd
7	Me	MTBE	30	90
8	Ph	CH ₂ Cl ₂	0	Nd
9	Bn	CH ₂ Cl ₂	0	Nd

^aReaction conditions: 3a (0.2 mmol), chloroformate reagent (2.0 equiv), EtMgBr (2.0 equiv), ligand L1 (6 mol %), and CuBr·SMe₂ (5 mol %) in solvent (2 mL). ^bThe reported yields correspond to isolated yields. ^cThe ee was determined by HPLC on a chiral stationary phase.

Also, 4-methoxyquinoline 3e shows potential for this catalytic system, providing product 4e with 75% yield and 97% ee, whereas 2-phenyl- and 2-bromo-4-methoxypyridines 3f and 3g did not result in any conversion. Finally, a substituent at the 3-position of the methoxypyridine was also tolerated, providing the corresponding product 4h with 62% yield and 82% ee.

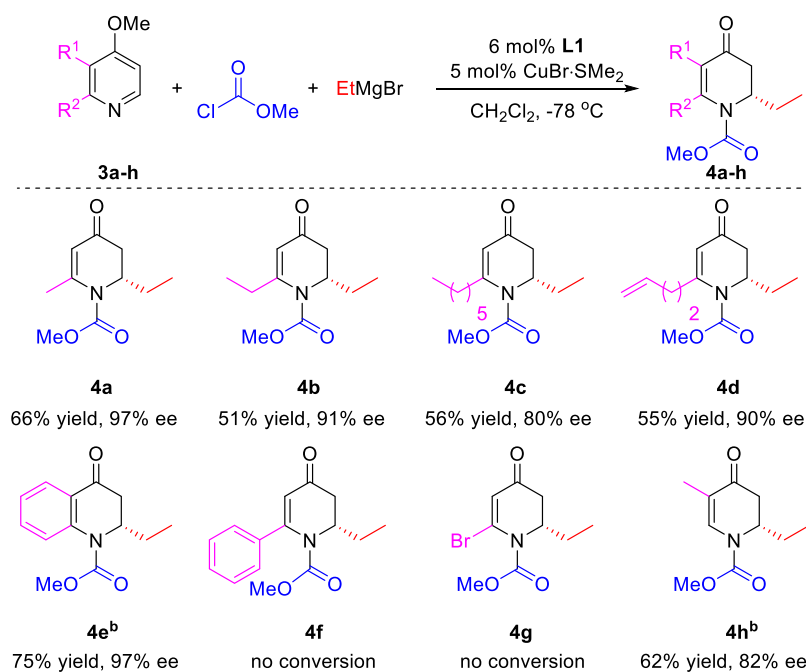
To demonstrate the utility of our catalytic system, a gram-scale reaction was performed, using only 1 mol % of the catalyst, maintaining 68% yield and 97% ee in the formation of

product 4a (Scheme 5a). Furthermore, the products accessed in this work are important building blocks for the synthesis of alkaloids. For example, our method allows access to compound 2q, which upon deprotection gives product 5, a key compound in the synthesis of Barrenazine A and B (Scheme 5b).⁸ Other examples are the synthesis of alkaloid precursor 6 with 92% yield as single trans diastereoisomer after hydrogenation⁹ and the synthesis of product 7, a crucial precursor to access the natural product (–)-epimyrine (Scheme 5c).¹⁰

To gain more insights into the origin of the stereoselectivity, we have initially conducted density functional theory calculations.¹¹ In line with the experimental data, we posit that the overall transformation consists of two stages: (i) formation of a pyridinium ion upon acylation and (ii) interaction of the resulting salt with the chiral copper complex, leading to the final chiral product.

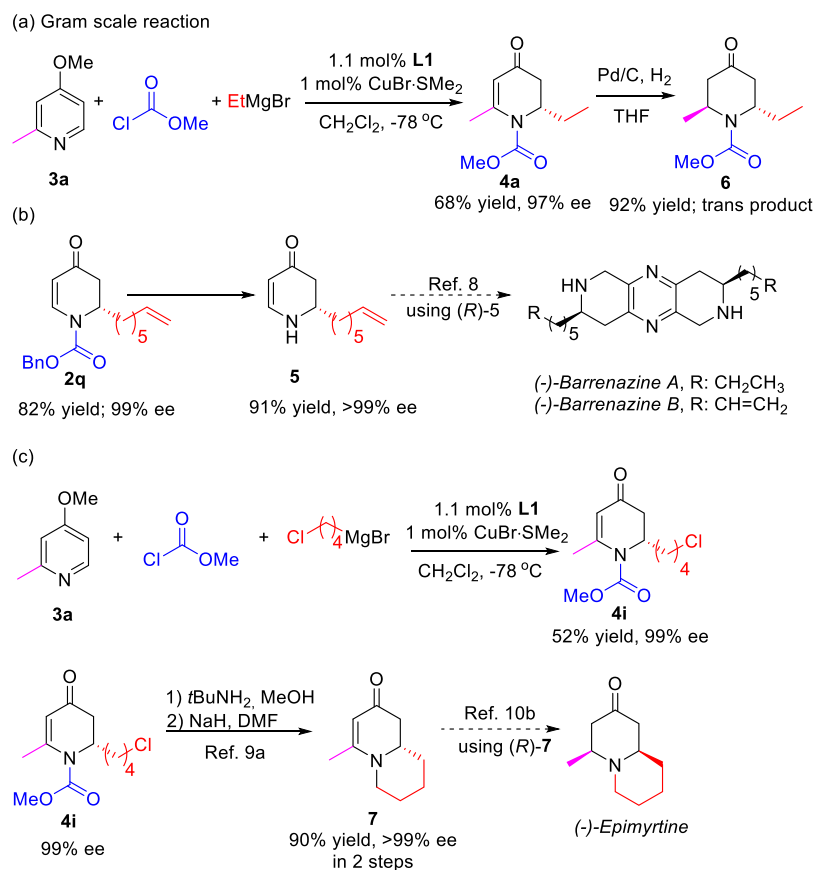
For the computational studies, we selected CuBr in combination with L1 as the chiral copper complex, 4-methoxy-2-methylpyridine 3a activated with methyl chloroformate as the substrate, and EtMgBr·2Et₂O as the Grignard reagent. Prior to the exploration of the reaction of the acylpyridinium salt with the Grignard reagent in the presence of the copper catalyst, we explored the direct addition of the Grignard reagent to II. We found that the activation energy for the direct addition of the Grignard reagent to II is 14.70 kcal/mol (Figure S3). Then, we explored the copper salt speciation in the presence of ligand L1 and the Grignard reagent.

We found that both the formation of the L1–CuBr complex from [Cu₂Br₂(SMe₂)₂] and the subsequent transmetalation upon addition of EtMgBr leading to organocopper species L1–CuEt are highly exergonic processes ($\Delta G = -37.90$ and -39.21 kcal/mol, respectively, Figure S4). With this in mind, we envisioned that the resulting organocopper species L1–CuEt can coordinate to II either via the carbonyl moiety,

Scheme 4. Scope of 4-Methoxypyridine Derivatives as Substrates^a

^aReaction conditions are the same as in Table 2, using different substituted 4-methoxypyridines. The reported yields correspond to isolated yields. ^bL1 (12 mol %) and CuBr·SMe₂ (10 mol %) were used.

Scheme 5. Synthetic Applications of the Methodology



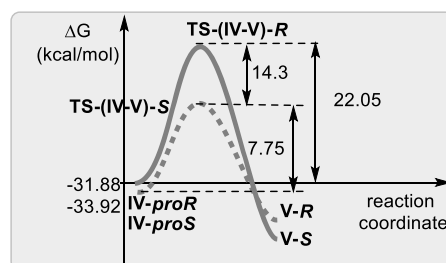
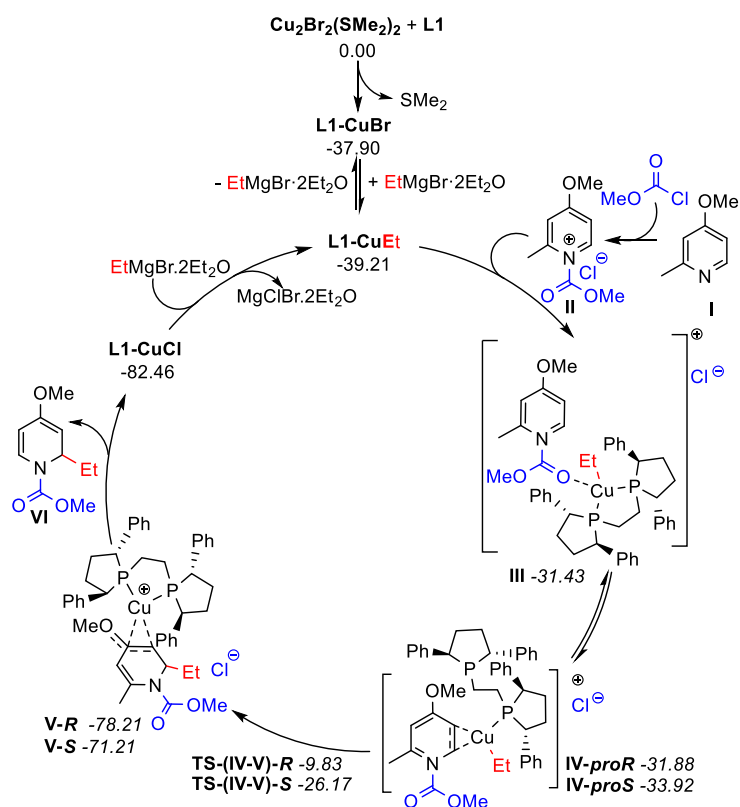
yielding **III**, or via the pyridine ring, specifically at position C-5-C-6, rendering **IV**. These two species are very close in energy and therefore likely in equilibrium. For the formation of **IV**, the coordination of the metallic center to the substrate is accompanied by the release of one of the phosphine groups at the ligand from the copper center in order to allow copper to accommodate the pyridinium substrate in its first coordination sphere (Scheme 6a). Although decoordination of the phosphine moiety is enthalpically disfavored, this is partially balanced by the coordination of the substrate to the copper center. At this point, the delivery of the *Et* group from the copper complex to the substrate can take place from complexes **III** or **IV**. However, the path from **III** toward the product is energetically more demanding than that from **IV** (Scheme S1). Therefore, continuing with complex **IV**, the approach of the copper can take place on either side of the two faces of the pyridine ring. Our calculations show that the *proS* diastereomeric complex is 2.04 kcal/mol more stable than the *proR* counterpart. Once species **IV-proS** is formed, it can further progress via nucleophilic addition of the ethyl moiety to form species **V**. The release of *Et* is facilitated by the approach of the dangling phosphorous to the metallic center, which ensures that the copper center remains tetracoordinated in this step. The evolution of **IV-proS** toward **V-S** involves a transition state with an activation energy of 7.75 kcal/mol, whereas the analogous transition state in the case of **IV-proR** involves an activation energy of 22.05 kcal/mol, rendering it non-competitive under the working conditions. The striking energy difference between these two transition states can be rationalized from the analysis of their structures (Scheme 6c). In **TS-(IV-V)-R**, one of the P-Cu bonds is significantly

elongated ($d_{\text{Cu-P-5}} = 3.38 \text{ \AA}$) in order to accommodate the substrate. The reason behind the need of dissociation of the phosphorous atom resides in the clash between one of the phenyl rings of the ligand and the substrate. On the contrary, in the **TS-(IV-V)-S**, the phenyl group is now replaced by a hydrogen atom, thus significantly reducing the steric interaction between the substrate and the substituents in the ligand. Furthermore, the weakening of one of the phosphorous-copper bonds at **TS-(IV-V)-R** results in slightly shortened Cu-C bond distances ($d_{\text{Cu-C-5}} = 2.13 \text{ \AA}$ and $d_{\text{Cu-C-6}} = 2.14 \text{ \AA}$), creating an earlier and also energetically more demanding transition state. Once *Et* is transferred from the organocopper to the 4-methoxy-2-methyl-pyridine, the counterion can behave as a new ligand, yielding **V** (R : -78.21 and S : -71.21 kcal/mol). In **V**, the interaction between the metal and the substrate at position 5 (Scheme 6a) is very weak, particularly in **V-S** ($d_{\text{Cu-C-5(V-R)}} = 2.16 \text{ \AA}$ and $d_{\text{Cu-C-5(V-S)}} = 2.40 \text{ \AA}$), and the breaking of this complex is very favorable ($\Delta G_{\text{L1-CuCl}} = -82.46$ kcal/mol). The release of the **L1-CuCl** complex ensures a new catalytic cycle.

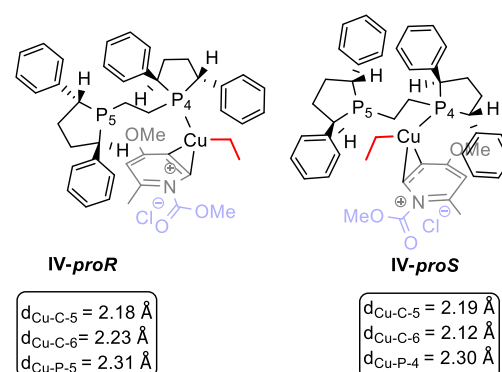
The computational data highlight the importance of the bidentate character of ligand **L1**, as well as the presence of a flexible linkage between the two phosphine moieties in its structure for the reactivity of the catalytic system and its enantiodifferentiating ability. To corroborate these results experimentally, we synthesized three chiral ligands **L8-L10** (Scheme 6d) that lack either the flexible linkage (**L8** and **L9**) or have a less pronounced bidentate character (**L9** and **L10**). These ligands were tested in combination with Cu(I) salt in the reaction of the synthesis of **2d** under optimized reaction conditions. In stark contrast to the results obtained with **L1**

Scheme 6. Proposed Mechanism for the Cu-Catalyzed Enantioselective Addition of Grignard Reagents to Substrate 1a^a

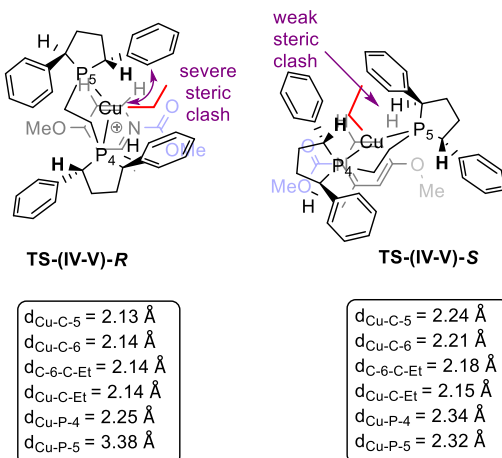
(a) Proposed mechanism for the Cu-catalyzed reaction



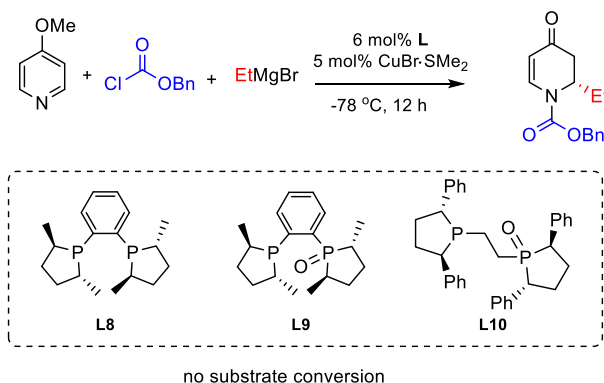
(b) Structural analysis of IV



(c) Structural analysis of the transition states TS-(IV-V)



(d) Catalysis data using chiral ligands L7-L9 in combination with Cu(I)



^aCalculations were performed at the $\text{PCM}(\text{CH}_2\text{Cl}_2)^{12}/\text{B3LYP-D3}/\text{def2tzvpp}/\text{B3LYP-D3}/\text{def2svp}^{13}$ computational level using the Gaussian 09 program.¹⁴ The thermochemistry was obtained at 1 atm and 298.15 K. The pyridinium species and the **L1** ligand are depicted in black, the protecting group in blue, and the ethyl group in red. (a) Left: proposed reaction mechanism. Right: reaction profile of the diastereoselective-determining step. (b) Structural analysis of the minima **IV** (*proR* and *proS*). (c) Structural analysis of the transition states **TS-(IV-V)**. For visualization purposes, additional color coding is used in sections (b) and (c), showing the pyridinium species in light gray and blue, the **L1** ligand in black, and the ethyl group in red. (d) Results of the catalytic addition of EtMgBr to **1a** using **Cu(I)** salt in combination with chiral ligands **L8-L10** under optimized reaction conditions.

(Scheme 3), no substrate conversion was observed when ligands **L8-L10** were used. Next, we carried out NMR spectroscopic studies of the copper complexes formed upon mixing of the copper salt with chiral ligands **L9** and **L10**, aiming to see the binding mode of these mono-oxidized ligands to copper (Figures S6 and S7 in Supporting Information). The results obtained confirmed the bidentate complexation of the rigid mono-oxidized ligand **L9** to the copper, while mono-oxidized ligand **L10** with the flexible link behaved as a

monodentate ligand. In an attempt to further understand the influence of the binding angle and the ligand rigidity, we recomputed the stereo-determining step using **L8** (Scheme S2) and found that enantiodiscrimination is in principle possible, but that the difference in energy between the paths leading to the *R* and *S* enantiomers of the product is smaller than that in the case when using our optimal catalyst (with ligand **L1**). The less pronounced enantiodiscrimination is caused by the rigidity of the ligand that impedes the release of one of the phosphine

arms. Importantly, the energy of the complexes **IV** with this ligand, as well as the subsequent transition states, is quite high, explaining the fruitless attempts to make this reaction work experimentally and emphasizing the importance of flexible bidentate ligands for the current transformation.

In conclusion, we have developed highly efficient catalytic asymmetric addition of Grignard reagents to in situ-formed *N*-acylpyridinium salts, with high yields and ees. The reaction is operationally simple and tolerates a wide range of pyridine derivatives and Grignard reagents and thus has a potential for applications in the synthesis of alkaloids and other complex building blocks. Finally, mechanistic studies revealed that certain structural motives, namely, the bidentate character and the flexible linkage between two binding arms, are responsible for the reactivity of the catalyst and for the transfer of chiral information from the catalyst to the final product.

■ ASSOCIATED CONTENT

SI Supporting Information

The Supporting Information is available free of charge at <https://pubs.acs.org/doi/10.1021/acscatal.1c01544>.

General experimental protocols, mechanistic studies, and full characterization of all the species reported; ¹H NMR and ¹³C NMR spectra of all the reported compounds; HPLC traces and HRMS data of new compounds; computational details; electronic energies; stability and imaginary frequencies of each stationary point; and Cartesian coordinates (PDF)

■ AUTHOR INFORMATION

Corresponding Author

Syuzanna R. Harutyunyan – *Stratingh Institute for Chemistry, University of Groningen, Groningen 9747 AG, The Netherlands*; orcid.org/0000-0003-2411-1250;
Email: s.harutyunyan@rug.nl

Authors

Yafei Guo – *Stratingh Institute for Chemistry, University of Groningen, Groningen 9747 AG, The Netherlands*

Marta Castiñeira Reis – *Stratingh Institute for Chemistry, University of Groningen, Groningen 9747 AG, The Netherlands*

Johanan Kootstra – *Stratingh Institute for Chemistry, University of Groningen, Groningen 9747 AG, The Netherlands*

Complete contact information is available at:
<https://pubs.acs.org/10.1021/acscatal.1c01544>

Notes

The authors declare no competing financial interest.

■ ACKNOWLEDGMENTS

Financial support from the European Research Council (S.R.H. grant no. 773264, LACOPAROM), The Netherlands Organization for Scientific Research (NWO-VICI to S.R.H.), and the China Scholarship Council (CSC, to Y.G.) are acknowledged. M.C.R. thanks the Centro de Supercomputación de Galicia (CESGA) for the free allocation of computational resources and the Xunta de Galicia (Galicia, Spain) for financial support through the ED481B-Axudas de apoio á etapa de formación posdoutoral (modalidade A) fellowship.

■ REFERENCES

- (1) (a) Vitaku, E.; Smith, D. T.; Njardarson, J. T. Analysis of the Structural Diversity, Substitution Patterns, and Frequency of Nitrogen Heterocycles among U.S. FDA Approved Pharmaceuticals. *J. Med. Chem.* **2014**, *57*, 10257–10274. (b) Kiuru, P.; Yli-Kauhala, J. *Pyridine and its Derivatives in Heterocycles in Natural Product Synthesis*; Majumdar, K. C., Chattopadhyay, S. K., Eds.; Wiley-VCH: Weinheim, 2011. Vol. 8, Chapter 8, pp. 267–297; (c) Escolano, C.; Amat, M.; Bosch, J. Chiral Oxazolopiperidone Lactams: Versatile Intermediates for the Enantioselective Synthesis of Piperidine-Containing Natural Products. *Chem.—Eur. J.* **2006**, *12*, 8198–8207. (d) Ma, X.; Gang, D. R. The Lycopodium Alkaloids. *Nat. Prod. Rep.* **2004**, *21*, 752–772. (e) Stout, D. M.; Meyers, A. I. Recent Advances in the Chemistry of Dihydropyridines. *Chem. Rev.* **1982**, *82*, 223–243.
- (2) (a) Sánchez-Roselló, M.; Acuña, J. L.; Simón-Fuentes, A.; del Pozo, C. A General Overview of the Organocatalytic Intramolecular aza-Michael reaction. *Chem. Soc. Rev.* **2014**, *43*, 7430–7453. (b) Kobayashi, S.; Komiyama, S.; Ishitani, H. The First Enantioselective Aza-Diels-Alder Reactions of Imino Dienophiles on Use of a Chiral Zirconium Catalyst. *Angew. Chem., Int. Ed.* **1998**, *37*, 979–981. (c) Yu, J.; Shi, F.; Gong, L.-Z. Brønsted-Acid-Catalyzed Asymmetric Multicomponent Reactions for the Facile Synthesis of Highly Enantioenriched Structurally Diverse Nitrogenous Heterocycles. *Acc. Chem. Res.* **2011**, *44*, 1156–1171. (d) Hussain, M.; Banchelin, T. S.-L.; Andersson, H.; Olsson, R.; Almqvist, F. Enantioselective Synthesis of Substituted Piperidines by Addition of Aryl Grignard Reagents to Pyridine *N*-Oxides. *Org. Lett.* **2013**, *15*, 54–57. (e) Andersson, H.; Gustafsson, M.; Boström, D.; Olsson, R.; Almqvist, F. The Regio- and Stereoselective Synthesis of trans-2,3-Dihydropyridine-*N*-oxides and Piperidines. *Angew. Chem., Int. Ed.* **2009**, *48*, 3288–3291. (f) Gribble, M. W., Jr; Liu, R. Y.; Buchwald, S. L. Evidence for Simultaneous Dearomatization of Two Aromatic Rings under Mild Conditions in Cu(I)-Catalyzed Direct Asymmetric Dearomatization of Pyridine. *J. Am. Chem. Soc.* **2020**, *142*, 11252–11269.
- (3) (a) Zheng, C.; You, S.-L. Transfer Hydrogenation with Hantzsch Esters and Related Organic Hydride Donors. *Chem. Soc. Rev.* **2012**, *41*, 2498–2518. (b) Yang, Z.-P.; Wu, Q.-F.; Shao, W.; You, S.-L. Iridium-Catalyzed Intramolecular Asymmetric Allylic Dearomatization Reaction of Pyridines, Pyrazines, Quinolines, and Isoquinolines. *J. Am. Chem. Soc.* **2015**, *137*, 15899–15906. (c) Ding, Q.; Zhou, X.; Fan, R. Recent Advances in Dearomatization of Heteroaromatic Compounds. *Org. Biomol. Chem.* **2014**, *12*, 4807–4815. (d) Gribble, M. W., Jr; Guo, S.; Buchwald, S. L. Asymmetric Cu-Catalyzed 1,4-Dearomatization of Pyridines and Pyridazines without Preactivation of the Heterocycle or Nucleophile. *J. Am. Chem. Soc.* **2018**, *140*, 5057–5060. (e) Bertuzzi, G.; Bernardi, L.; Fochi, M. Nucleophilic Dearomatization of Activated Pyridines. *Catalysts* **2018**, *8*, 632–665.
- (4) (a) Shintani, R.; Tokunaga, N.; Doi, H.; Hayashi, T. A New Entry of Nucleophiles in Rhodium-Catalyzed Asymmetric 1,4-Addition Reactions: Addition of Organozinc Reagents for the Synthesis of 2-Aryl-4-Piperidones. *J. Am. Chem. Soc.* **2004**, *126*, 6240–6241. (b) Müller, D.; Alexakis, A. Copper-Catalyzed Asymmetric 1,4-Addition of Alkenyl Alanes to *N*-Substituted-2,3-Dehydro-4-Piperidones. *Org. Lett.* **2012**, *14*, 1842–1845. (c) Jagt, R. B. C.; de Vries, J. G.; Feringa, B. L.; Minnaard, A. J. Enantioselective Synthesis of 2-Aryl-4-Piperidones via Rhodium/Phosphoramidite-Catalyzed Conjugate Addition of Arylboroxines. *Org. Lett.* **2005**, *7*, 2433–2435. (d) Xu, Q.; Zhang, R.; Zhang, T.; Shi, M. Asymmetric 1,4-Addition of Arylboronic Acids to 2,3-Dihydro-4-pyridones Catalyzed by Axially Chiral NHC–Pd(II) Complexes. *J. Org. Chem.* **2010**, *75*, 3935–3937. (e) Sebesta, R.; Pizzuti, M. G.; Boersma, A. J.; Minnaard, A. J.; Feringa, B. L. Catalytic Enantioselective Conjugate Addition of Dialkylzinc Reagents to *N*-Substituted-2,3-Dehydro-4-Piperidones. *Chem. Commun.* **2005**, 1711–3. (f) Pizzuti, M. G.; Minnaard, A. J.; Feringa, B. L. Catalytic Asymmetric Synthesis of the Alkaloid (+)-Myrtine. *Org. Biomol. Chem.* **2008**, *6*, 3464–3466. (g) Guo, F.; Dhakal, R. C.; Dieter, R. K. Conjugate Addition Reactions of *N*-Carbamoyl-4-Pyridones and 2,3-Dihydropyridones

with Grignard Reagents in the Absence of Cu(I) salts. *J. Org. Chem.* **2013**, *78*, 8451–8464. (h) Dieter, R. K.; Guo, F. Conjugate Addition Reactions of *N*-Carbamoyl-4-Pyridones with Organometallic Reagents. *J. Org. Chem.* **2009**, *74*, 3843–3848. (i) Guo, Y.; Harutyunyan, S. R. Highly Enantioselective Catalytic Addition of Grignard Reagents to *N*-Heterocyclic Acceptors. *Angew. Chem., Int. Ed.* **2019**, *58*, 12950–12954.

(5) (a) Tsukanov, S. V.; Marks, L. R.; Comins, D. L. Studies Toward the Synthesis of Lepadiformine A. *J. Org. Chem.* **2016**, *81*, 10433–10443. (b) Tsukanov, S. V.; Comins, D. L. Concise Total Synthesis of the Frog Alkaloid (–)-205 B. *Angew. Chem., Int. Ed.* **2011**, *50*, 8626–8628. (c) Comins, D. L.; Kueth, J. T.; Hong, H.; Lakner, F. J.; Concolino, T. E.; Rheingold, A. L. Diastereoselective Addition of Prochiral Metallo Enolates to Chiral 1-Acylpyridinium Salts. *J. Am. Chem. Soc.* **1999**, *121*, 2651–2652. (d) Comins, D. L.; Joseph, S. P.; Goehring, R. R. Asymmetric Synthesis of 2-Alkyl(Aryl)-2,3-dihydro-4-pyridones by Addition of Grignard Reagents to Chiral 1-Acyl-4-methoxypyridinium Salts. *J. Am. Chem. Soc.* **1994**, *116*, 4719–4728. (e) Charette, A. B.; Grenon, M.; Lemire, A.; Pourashraf, M.; Martel, J. Practical and Highly Regio- and Stereoselective Synthesis of 2-Substituted Dihydropyridines and Piperidines: Application to the Synthesis of (–)-Coniine. *J. Am. Chem. Soc.* **2001**, *123*, 11829–11830. (f) Legault, C.; Charette, A. B. Complexation Promoted Additions to *N*-Benzoyliminopyridinium Ylides. A Novel and Highly Regioselective Approach to Polysubstituted Piperidines. *J. Am. Chem. Soc.* **2003**, *125*, 6360–6361. (g) Hoesl, C. E.; Maurus, M.; Pabel, J.; Polborn, K.; Wanner, K. T. Generation of Chiral *N*-Acylpyridinium Ions by Means of Silyl Triflates and their Diastereoselective Trapping Reactions: Formation of *N*-Acyl-dihydropyridines and *N*-Acyl-dihydropyridones. *Tetrahedron* **2002**, *58*, 6757–6770.

(6) (a) García Mancheño, O.; Asmus, S.; Zurro, M.; Fischer, T. Highly Enantioselective Nucleophilic Dearomatization of Pyridines by Anion-Binding Catalysis. *Angew. Chem., Int. Ed.* **2015**, *54*, 8823–8827. (b) Sun, Z.; Yu, S.; Ding, Z.; Ma, D. Enantioselective Addition of Activated Terminal Alkynes to 1-Acylpyridinium Salts Catalyzed by Cu–Bis(oxazolone) Complexes. *J. Am. Chem. Soc.* **2007**, *129*, 9300–9301. (c) Ichikawa, E.; Suzuki, M.; Yabu, K.; Albert, M.; Kanai, M.; Shibasaki, M. New Entries in Lewis Acid–Lewis Base Bifunctional Asymmetric Catalyst: Catalytic Enantioselective Reissert Reaction of Pyridine Derivatives. *J. Am. Chem. Soc.* **2004**, *126*, 11808–11809. (d) Bertuzzi, G.; Sinisi, A.; Caruana, L.; Mazzanti, A.; Fochi, M.; Bernardi, L. Catalytic Enantioselective Addition of Indoles to Activated *N*-Benzylpyridinium Salts: Nucleophilic Dearomatization of Pyridines with Unusual C-4 Regioselectivity. *ACS Catal.* **2016**, *6*, 6473–6477. (e) Nadeau, C.; Aly, S.; Belyk, K. Rhodium-Catalyzed Enantioselective Addition of Boronic Acids to *N*-Benzylnicotinate Salts. *J. Am. Chem. Soc.* **2011**, *133*, 2878–2880. (f) Robinson, D. J.; Spurlin, S. P.; Gorden, J. D.; Karimov, R. R. Enantioselective Synthesis of Dihydropyridines Containing Quaternary Stereocenters through Dearomatization of Pyridinium Salts. *ACS Catal.* **2020**, *10*, 51–55. (h) Chau, S. T.; Lutz, J. P.; Wu, K.; Doyle, A. G. Nickel-Catalyzed Enantioselective Arylation of Pyridinium Ions: Harnessing an Iminium Ion Activation Mode. *Angew. Chem., Int. Ed.* **2013**, *52*, 9153–9156. (i) Lutz, J. P.; Chau, S. T.; Doyle, A. G. Nickel-Catalyzed Enantioselective Arylation of Pyridine. *Chem. Sci.* **2016**, *7*, 4105–4109. (j) Ángeles Fernández-Ibáñez, M.; Maciá, B.; Pizzuti, M. G.; Minnaard, A. J.; Feringa, B. L. Catalytic Enantioselective Addition of Dialkylzinc Reagents to *N*-Acylpyridinium Salts. *Angew. Chem., Int. Ed.* **2009**, *48*, 9339–9341.

(7) (a) Rodríguez-Fernández, M.; Yan, X.; Collados, J. F.; White, P. B.; Harutyunyan, S. R. Lewis Acid Enabled Copper-Catalyzed Asymmetric Synthesis of Chiral β -Substituted Amides. *J. Am. Chem. Soc.* **2017**, *139*, 14224–14231. (b) Yan, X.; Harutyunyan, S. R. Catalytic Enantioselective Addition of Organometallics to Unprotected Carboxylic Acids. *Nat. Commun.* **2019**, *10*, 3402. (c) Yan, X.; Ge, L.; Castiñeira Reis, M.; Harutyunyan, S. R. Nucleophilic Dearomatization of *N*-Heteroaromatics Enabled by Lewis Acids and Copper Catalysis. *J. Am. Chem. Soc.* **2020**, *142*, 20247–20256.

(8) Martínez, M. M.; Sarandeses, L. A.; Sestelo, J. P. Enantioselective synthesis of (–)-barrenazines A and B. *Tetrahedron Lett.* **2007**, *48*, 8536–8539.

(9) Gouault, N.; Le Roch, M.; de Campos Pinto, G.; David, M. Total Synthesis of Dendrobate Alkaloid (+)-241D, Isosolenopsin and Isosolenopsin A: Application of a Gold-Catalyzed Cyclization. *Org. Biomol. Chem.* **2012**, *10*, 5541–5546.

(10) (a) Suárez-Castillo, O. R.; Montiel-Ortega, L. A.; Meléndez-Rodríguez, M.; Sánchez-Zavala, M. Cleavage of Alkoxy carbonyl Protecting Groups from Carbamates by *t*-BuNH₂. *Tetrahedron Lett.* **2007**, *48*, 17–20. (b) Yang, Y. Building Polyfunctional Piperidines: a Stereoselective Strategy of a Three-component Mannich reaction Inspired by Biosynthesis and Applications in the Synthesis of Natural Alkaloids (+)-241D; (–)-241D; Isosolenopsin A and (–)-Epimyrine. *RSC Adv.* **2015**, *5*, 18894–18908.

(11) Kohn, W.; Sham, L. J. Self-Consistent Equations Including Exchange and Correlation Effects. *J. Phys. Rev.* **1965**, *140*, A1133.

(12) Tomasi, J.; Mennucci, B.; Cammi, R. Quantum Mechanical Continuum Solvation Models. *Chem. Rev.* **2005**, *105*, 2999–3094.

(13) (a) Becke, A. D. Density-functional Thermochemistry. III. The role of Exact Exchange. *J. Chem. Phys.* **1993**, *98*, 5648–5652.

(b) Becke, A. D. A New Mixing of Hartree-Fock and Local Density-Functional Theories. *J. Chem. Phys.* **1993**, *98*, 1372–1377. (c) Lee, C.; Yang, W.; Parr, R. G. Development of the Colle-Salvetti Correlation-Energy Formula into a Functional of the Electron Density. *Phys. Rev. B: Condens. Matter Mater. Phys.* **1988**, *37*, 785–789. (d) Weigend, F.; Ahlrichs, R. Balanced Basis Sets of Split Valence, Triple Zeta Valence and Quadruple Zeta Valence Quality for H to Rn: Design and Assessment of Accuracy. *Phys. Chem. Chem. Phys.* **2005**, *7*, 3297–3305.

(14) Frisch, M. J.; Trucks, G. W.; Schlegel, H. B.; Scuseria, G. E.; Robb, M. A.; Cheeseman, J. R.; Scalmani, G.; Barone, V.; Petersson, G. A.; Nakatsuji, H.; Li, X.; Caricato, M.; Marenich, A. V.; Bloino, J.; Janesko, B. G.; Gomperts, R.; Mennucci, B.; Hratchian, H. P.; Ortiz, J. V.; Izmaylov, A. F.; Sonnenberg, J. L.; Williams-Young, D.; Ding, F.; Lipparini, F.; Egidi, F.; Goings, J.; Peng, B.; Petrone, A.; Henderson, T.; Ranasinghe, D.; Zakrzewski, V. G.; Gao, J.; Rega, N.; Zheng, G.; Liang, W.; Hada, M.; Ehara, M.; Toyota, K.; Fukuda, R.; Hasegawa, J.; Ishida, M.; Nakajima, T.; Honda, Y.; Kitao, O.; Nakai, H.; Vreven, T.; Throssell, K.; Montgomery, Jr, J. A.; Peralta, J. E.; Ogliaro, F.; Bearpark, M. J.; Heyd, J. J.; Brothers, E. N.; Kudin, K. N.; Staroverov, V. N.; Keith, T. A.; Kobayashi, R.; Normand, J.; Raghavachari, K.; Rendell, A. P.; Burant, J. C.; Iyengar, S. S.; Tomasi, J.; Cossi, M.; Millam, J. M.; Klene, M.; Adamo, C.; Cammi, R.; Ochterski, J. W.; Martin, R. L.; Morokuma, K.; Farkas, O.; Foresman, J. B.; Fox, D. J. *Gaussian 09*; Gaussian, Inc.: Wallingford, CT, 2009.